ACS imaging of 25 galaxies in nearby groups and in the field

Igor D. Karachentsev

Special Astrophysical Observatory, Russian Academy of Sciences, N. Arkhyz, KChR, 369167, Russia

ikar@luna.sao.ru

Andrew Dolphin

Steward Observatory, 933 N. Cherry Ave., Tucson, AZ 85721

R. Brent Tully

University of Hawaii

Margarita Sharina, Lidia Makarova and Dmitry Makarov

Special Astrophysical Observatory, Russian Academy of Sciences, N. Arkhyz, KChR, 369167, Russia

Valentina Karachentseva

Astronomical Observatory of Kiev University, Kiev, Ukraine

Shoko Sakai

University of California - Los Angeles USA

Edward J. Shaya

U. of Maryland, Astronomy Dept. - College Park MD, USA

ABSTRACT

We present HST/ACS images and color-magnitude diagrams for 25 nearby galaxies with radial velocities $V_{LG} < 500 \text{ km s}^{-1}$. Distances are determined based on the luminosities of stars at the tip of the red giant branch that range from 2 Mpc to 12 Mpc. Two of the galaxies, NGC 4163 and IC 4662, are found to be the nearest known representatives of blue compact dwarf (BCD) objects.

Using high-quality data on distances and radial velocities of 110 nearby field galaxies, we derive their mean Hubble ratio to be $68 \text{ km s}^{-1} \text{ Mpc}^{-1}$ with standard

deviation of 15 km s⁻¹ Mpc⁻¹. Peculiar velocities of most of the galaxies, $V_{pec} = V_{LG} - 68D$, follow a Gaussian distribution with $\sigma_v = 63$ km s⁻¹, but with a tail towards high negative values. Our data displays the known correlation between peculiar velocity and galaxy elevation above the Local Supercluster plane. The small observed fraction of galaxies with high peculiar velocities, $V_{pec} < -500$ km s⁻¹, may be understood as objects associated with nearby groups (Coma I, Eridanus) outside the Local volume.

Subject headings: galaxies: distances – galaxies

1. Introduction

Until 2000, very little data have been available to describe the peculiar velocity field of galaxies around the Local Group. This surprising situation was caused by the lack of reliable data on distances (not velocities) for many of the nearest galaxies. The Local Group itself is in the highly nonlinear collapse regime. In a larger volume, deviations from pure Hubble expansion can be expected due to the gravitational action of nearby groups as well as by Virgo-centric and Great Attractor flows. Enormous progress has been made recently with accurate distance measurements of nearby galaxies beyond the Local Group based on the luminosity of the tip of the red giant branch (TRGB). This method (Lee et al. 1993) has a precision comparable to the Cepheid method (Sakai et al. 1996, Ferrarese et al. 2000, Sakai et al. 2004), but requires much less observing time. Over the last few years, WFPC2 snapshot surveys have made use of the TRGB method to obtain 10% distances for about 100 galaxies. Further significant progress is expected because the Advanced Camera for Surveys (ACS) probes about 1.5 mag deeper in an equal integration time and acquires a field double in area.

Apart from 36 members of the Local Group, there are, so far, 310 galaxies with distance estimates less than 7 Mpc. Among these, distances to 174 galaxies have been measured with an accuracy of 10% based on the Cepheid method (N=12), or the luminosity of the TRGB (N=162). A list of these galaxies is presented in "Catalog of Neighboring Galaxies" (CNG) by Karachentsev et al. (2004). The remaining galaxies have only rough distance estimates from the luminosity of their brightest stars, the Tully-Fisher relation, or from their membership in the known nearby groups. In this restricted distance range the TRGB method is most effective because it provides accurate distances to galaxies of all morphologies with minimal observational demands. The superior angular resolution of HST has been a critical factor: 95% of the TRGB distances have been obtained with HST during the last four years. The remaining 136 galaxies are suitable targets for a SNAP survey with the Advanced Camera

at HST.

The radial velocity – distance relation for nearby galaxies is shown in Figure 1. Within 7 Mpc there are two substantial groups of galaxies: around M 81 and Cen A. The average distances of 3.7 Mpc, and 3.8 Mpc, respectively, are very similar. Members of these two groups are shown in Figure 1 as open circles. The solid line corresponds to the Hubble relation with $H_0 = 68 \text{ km s}^{-1} \text{ Mpc}^{-1}$, curved at small distances because of the decelerating gravitational action of the Local Group (Lynden-Bell 1981, Sandage 1986) assuming a total mass of $1.3 \times 10^{12} M_{\odot}$. The largest deviations from the Hubble regression are seen to be related to the virial motions of galaxies inside the M81 and Cen A groups. An "S –wave" feature brackets the distance regime of the two dominant groups: nearer galaxies have velocities that exceed the Hubble flow and more distant galaxies have lower velocities. This pattern is the signature of infall toward massive attractors.

Karachentsev & Makarov (1996, 2001) found that the local expansion on a scale of 5 Mpc is significantly anisotropic, described by the tensor H_{ij} with values (81±3): (62±3): (48±5) in km s⁻¹. The minor axis of the ellipsoid is directed towards the pole of the Local Supercluster, and the major axis has an angle of (29±5)° with respect to the direction of the Virgo Cluster (shifted towards the Great Attractor position). Later, Karachentsev et al. (2003) have used TRGB distances derived with WFPC2 data to confirm the local velocity anisotropy. Some galaxies in Figure 1 (like UGC 3755) that lie well below the Hubble line are all found at high supergalactic latitudes. Given the observed concentration of nearby galaxies to the Supergalactic equatorial plane, the retardation from Hubble flow seen in the high latitude galaxies is expected. It follows naturally from numerical action models of large scale flows (Shaya, Peebles, & Tully 1995) where mass is assumed to be distributed like the light of all the known galaxies (in a census that extends to the Great Attractor).

The accurate distances that have already been obtained with the HST snap surveys provide tremendous new constraints for numerical action modeling. It is to be appreciated that peculiar motions are best constrained locally. A 10% error at a Hubble distance of $300~\rm km~s^{-1}$ translates to an uncertainty in peculiar velocity of only $30~\rm km~s^{-1}$ but the error increases linearly with distance. Every accurate distance provides an additional constraint on the local distribution of matter. The widest possible coverage of the sky is desired.

According to the results of N-body simulations (Governato et al. 1997, Massio et al. 2005) the dispersion in the motions of field galaxies and group centers around the mean flow, σ_v , contains information on galaxy formation, the density of matter, Ω_m , and the relative importance of Dark Energy, Ω_{λ} . Early hints of a cold local Hubble flow (Sandage et al. 1972, Tully 1982) have been confirmed by the results of HST TRGB programs (Karachentsev et al. 2003c). Galaxies within 3 Mpc of the Local Group yield a surprisingly low dispersion, σ_v

about 25 – 30 km s⁻¹, and the dispersion of the centroids of the nearest groups (Local, M 81, IC 342, Scl, Centaurus A, M 83, Canes Venatici I groups) is ~25 km s⁻¹. Quiescence of the local Hubble flow is a signature of a vacuum-dominated universe (Chernin 2001, Baryshev et al. 2001). Cosmological simulations based on the Cold Dark Matter (CDM) paradigm but without Dark Energy inevitably produce models with local random motions that are too high. Maccio et al. (2005) show that CDM models with Dark Energy can result in low random motions in the density regime of the local neighborhood. The earlier in history the transition from the dominance of attraction to the dominance of repulsion, the lower the random motions expected today due to the enhanced effect of adiabatic cooling with expansion.

2. HST ACS photometry

Our sample consists of 25 galaxies observed with the Advanced Camera for Surveys (ACS) as part of an HST Cycle 12 snapshot project (#9771). We obtained 1200s F606W and 900s F814W images of each galaxy using ACS/WFC with a CR-split of two. The cosmic ray cleaned images (CRJ data sets) were obtained from the STScI archive, having been processed according to the standard ACS pipeline.

Stellar photometry was obtained using the ACS module of DOLPHOT (Dolphin et al. in prep), using the recommended recipe and parameters. In brief, this involves the following steps. First, pixels that are flagged as bad or saturated in the data quality images were marked in the data images. Second, pixel area maps were applied to restore the correct count rates. Finally, the photometry was run.

In order to be reported, a star had to be recovered with S/N of at least five in both filters, be relatively clean of bad pixels (such that the DOLPHOT flags are zero) in both filters, and pass our goodness of fit criteria ($\chi \leq 2.5$ and $|sharp| \leq 0.3$).

To estimate our photometric uncertainties and completeness, artificial star tests were run on the KK230 and NGC247 fields, which represent the most and least crowded images. Completeness plots are shown in Figure 2. We note that the plateau at $\sim 85\%$ completeness is due to bad pixels and cosmic rays. We also show the magnitude errors as a function of recovered magnitude in Figure 3.

CTE corrections were made according to ACS ISR03-09, and our zero points and transformations were made according to Sirianni et al. (2005). We estimate the uncertainties in the calibration to be 0.05 to 0.10 magnitudes.

We determined the TRGB using a Gaussian-smoothed I-band luminosity function for red stars with colors V-I within $\pm 0^{\rm m}5$ of the mean $\langle V-I \rangle$ expected for red giant branch stars. Following Sakai et al. (1996), we applied a Sobel edge-detection filter. The position of the TRGB was identified with the peak in the filter response function. According to Da Costa & Armandroff (1990), for metal-poor systems the TRGB is located at $M_I = -4.05$ mag. Ferrarese et al. (2000) calibrated the zero point of the TRGB from galaxies with Cepheid distances and estimated $M_I = -4^{\rm m}06 \pm 0^{\rm m}07(random) \pm 0.13(systematic)$. A new TRGB calibration, $M_I = -4^{\rm m}04 \pm 0^{\rm m}12$, was made by Bellazzini et al.(2001) based on photometry and on a distance estimate from a detached eclipsing binary in the Galactic globular cluster ω Centauri. For this paper (as for our previuos works with the HST data) we use $M_I = -4^{\rm m}05$.

3. TRGB distances and integrated properties

ACS images of 25 observed galaxies are shown in Figure 4. The compass in each field indicates the North and East directions. Usually our target galaxies were centered on the middle of the ACS field, but for two large targets (NGC 247, NGC 4605) the ACS position was shifted towards the galaxy periphery to decrease a stellar crowding effect. In Figure 5 I versus (V - I) color magnitude diagrams (CMDs) for the 25 galaxies are presented.

A summary of the resulting distance moduli for the observed galaxies is given in Table 1. Its columns contain: (1) galaxy name, (2) equatorial coordinates, (3) radial velocity in km s⁻¹ in the Local Group (LG) rest frame with the apex parameters from NASA Extragalactic Database (NED), (4) position of the TRGB in apparent I-band magnitude, (5) the total number of detected stars per image, (6) Galactic extinction in the I-band from Schlegel et al. (1998), (7) true distance modulus in mag, and (8) linear distance in Mpc. Taking into account the typical uncertainty in the TRGB ($\sim 0^{\text{m}}15$), as well as uncertainties of the HST photometry zero point ($\sim 0^{\text{m}}05$), the aperture corrections ($\sim 0^{\text{m}}05$), and the crowding effects ($\sim 0^{\text{m}}06$) added quadratically, we estimate the uncertainty in the derived distances to be about 8%.

Some additional comments about the galaxy properties are briefly discussed below. The galaxies are listed in order by increasing Right Acsention.

ESO 349-031= SDIG. This dIr galaxy belongs to a group (filament) in Sculptor. Its TRGB distance of 3.21 Mpc turns out to be 0.9 Mpc less than a former estimate derived from the Tully-Fisher (TF) relation by Karachentsev et al. (2003a). Judging from its distance and radial velocity, SDIG is a companion to bright spiral galaxy NGC 7793.

- NGC 247. Among the known galaxies in the Sculptor filament, this spiral galaxy remained the last one without reliable distance estimate. Dimensions of NGC 247 ($27' \times 7'$) extend far beyond the ACS field. We targeted the northern side of the galaxy at a distance of 6'.5 from the nucleus which is relatively free from bright stellar complexes. Nevertheless, about 1.7×10^5 stars have been detected in this field. The derived TRGB distance to NGC 247, 3.65 Mpc, agrees with the distance estimate, 4.1 Mpc, obtained from the TF-relation (Karachentsev et al. 2003a).
- **KKH 6.** According to its radial velocity and distance, this dIr galaxy is located at a far outskirt of the group around the galaxy pair Maffei 1 and Maffei 2. The structure of this group is strongly compromised by Galactic extinction.
- UGCA 86. This Magellanic type irregular galaxy with a prominent region of star formation (VII Zw 9) at its southern side has been imaged with WFPC2 by Karachentsev et al. (2003b), however, the former observations yield only the lower limit of its distance, D > 2.2 Mpc. Our present distance estimate, 2.96 Mpc, confirms the suggestion that UGCA 86 is a companion to the giant spiral IC 342 situated at a distance of 3.28 Mpc (Saha et al. 2002).
- UGCA 92. This irregular galaxy with low radial velocity, $V_{LG} = 89 \text{ km s}^{-1}$, is situated in a zone of strong extinction. Karachentsev et al. (1997) estimated its distance to be 1.8 Mpc based on the luminosity of brightest blue stars. With the new TRGB distance, 3.01 Mpc, the galaxy, as well as UGCA 86, turns out to be a physical member of the group around IC 342. Note that 75 arcmin away from UGCA 92 there is another galaxy, NGC 1569, of almost the same radial velocity $V_{LG} = 88 \text{ km s}^{-1}$. Makarova & Karachentsev (2003) carried out stellar photometry of two HST/WFPC2 fields at a far periphery of NGC 1569 and derived two possible distance estimates: $1.95\pm0.2 \text{ Mpc}$ and $2.8\pm0.2 \text{ Mpc}$. The second estimates agrees better with the new distance of UGCA 92.
- ESO 121-20 = KKs 19. This very isolated dIr galaxy was detected in the HI line by Huchtmeier et al. (2001). Its individual distance estimate, 6.05 Mpc, is derived by us for the first time. With this distance, the galaxy has a high hydrogen mass-to-luminosity ratio, $M(HI)/L_B = 2.9$ as well as high indicative mass-to-luminosity ratio, $M_{25}/L_B = 18.5$ in solar units that gives evidence of the existence around ESO 121–20 of an extended HI envelope like around some other isolated irregular galaxies: DDO 154 and NGC 3741 (Begum et al. 2005).
- KKH 37 = Mailyan 16. This dIr galaxy of low surface brightness is situated at the northern periphery of the IC 342 group. The TRGB distance to KKH 37, 3.39 Mpc, is just the same as to IC 342 and NGC 2403. In this obscured region of sky there may be other

dwarf galaxies, undetected so far, which fill the gap between the two groups around these bright spiral galaxies.

- **ESO 059-01.** This is an isolated irregular galaxy with a high indicative mass-to-luminosity ratio, $M_{25}/L_B = 15.2 M_{\odot}/L_{\odot}$ at the TRGB distance D = 4.57 Mpc.
- DDO 52 = UGC 4426. This dIr galaxy is very isolated. The nearest galaxy of normal luminosity, NGC 2683, is located about 2.5 Mpc away from DDO 52. The present case demonstrates to us that a galaxy of 10 Mpc distance is reachable with ACS in a single orbit SNAP observation.
- **D564-08.** This dIr galaxy of low surface brightness from a list of Taylor et al. (1996) is a probable distant companion to the giant spiral galaxy NGC 2903. Its radial velocity, $V_{LG} = 365 \text{ km s}^{-1}$ is surprisingly low for the distance of 8.67 Mpc, giving an individual Hubble ratio $H_i = 42 \text{ km s}^{-1} \text{ Mpc}^{-1}$. A similar low value, $H_i = 39 \text{ km s}^{-1} \text{ Mpc}^{-1}$, is also found for the isolated galaxy DDO 52 discussed above.
- **D634-03.** This is the most unusual object of low surface brightness from the list by Taylor et al. (1996). Its low radial velocity, $V_{LG} = 172 \text{ km s}^{-1}$ measured by Schombert et al. (1997) was later confirmed by Huchtmeier (personal communication), who derived $V_{LG} = 173 \text{ km s}^{-1}$, the HI line width $W_{50} = 34 \text{ km s}^{-1}$, and the HI flux $F = 0.25 \text{ Jy km s}^{-1}$. The RGB of D634-03 is not seen distinctly in its CM diagram. A probable position of the TRGB seems to be near $I = 25^{\text{m}}$ 9 which corresponds to the galaxy distance 9.46 Mpc. With an apparent total magnitude of $B = 17^{\text{m}}$ 5, D634-03 has an absolute magnitude of -12.54, the hydrogen mass-to-luminosity ratio $0.37 M_{\odot}/L_{\odot}$, and the total (indicative) mass-to-luminosity ratio $10 M_{\odot}/L_{\odot}$. An individual Hubble ratio of this isolated galaxy is only 18 km s⁻¹ Mpc⁻¹ indicating a high peculiar velocity.
- **D565-06.** One more galaxy of low surface brightness from Taylor et al. (1996). Its low radial velocity, $V_{LG} = 386 \text{ km s}^{-1}$, contrasts with the large TRGB distance, 9.08 Mpc. Based on this distance, D565-06 is a companion to NGC 2903, which has $V_{LG} = 442 \text{ km s}^{-1}$ and a distance of 8.9 Mpc from the luminosity of its brightest stars.
- **IKN.** This galaxy of very low surface brightness is a new dwarf spheroidal member of the M 81 group. IKN is situated 1' south from a bright star, mimicking the star reflex on POSS-II plates. Our ACS photometry reveals 2×10^4 stars seen in both filters. Most of them belong to RGB population. Near the center of IKN, we found a candidate globular cluster marked in Fig. 4 by a circle. From its dimension (2'.7) and apparent magnitude, $B_T = 16.0$, IKN resembles another dSph member of this group, F8D1 observed with WFPC2 by Caldwell et al. (1998).

- HS 117. This dwarf system was found by Huchtmeier & Skillman (1998), who detected it in the HI line with $V_h = -37 \text{ km s}^{-1}$, i.e. in the range of Galactic hydrogen emission. The CM diagram of HS 117 on Fig. 5 exhibits a distinct sequence of RGB stars as well as some number of bluish stars. Based on its optical and HI properties, HS 117 may be classified as a dwarf galaxy of the transition dIr/dSph type.
- NGC 4068. This blue dwarf galaxy belongs to the Canes Venatici I (CVn I) cloud. Makarova et al. (1997) estimated its distance via the brightest stars to be 0.9 Mpc greater than the new distance of 4.31 Mpc to NGC 4068 derived by us from the TRGB.
- NGC 4163. This is another blue and compact galaxy in the CVn I cloud. Its old distance, 3.6 Mpc, was estimated by Tikhonov & Karachentsev (1998) from the brightest stars. Our new estimate of 2.96 Mpc from the TRGB places NGC 4163 at the nearby edge of the CVn I cloud which makes it the second nearest BCD galaxy.
- UGC 7242 = KKH 77. A bright star projected into the northern side of this dIr galaxy renders stellar photometry of UGC 7242 to be incomplete. The galaxy is situated at the far outskirt of the M 81 group, behind the main body of the group.
- IC 779 = UGC 7369. This is a lenticular galaxy with a semi-stellar nucleus. Despite its low radial velocity, $V_{LG} = 198 \,\mathrm{km \ s^{-1}}$, IC 779 does not look to be a nearby object. For this reason it was excluded from the Local Volume galaxies (see Table 3 in CNG, Karachentsev et al. 2004). The distribution of the resolved red stars over the ACS area reveals that most are concentrated within the main optical boundary of the galaxy. The CM diagram of IC 779 in Fig.5 shows what might be an upper part of the RGB with the TRGB position at $I \sim 26^{\rm m}$. Alternatively, these stars might be part of the asymptotic giant branch (AGB). From its position on the sky, it is suspected that this galaxy is a member of the Coma I group. Assuming we are picking up the TRGB, the derived distance to IC 779 is 11.6 Mpc. The plausible association with the Coma I group would place the galaxy at 16 Mpc (Tonry et al. 2001) whence the TRGB would be lost at the $I \sim 27$ limit of our observations. This ambiguity created by AGB populations demonstrates the breakdown of the TRGB method near the photometric limit. In the case of single orbit observations with ACS of galaxies with young populations, the limit of reliable TRGB measures is $\sim 10 \,\mathrm{Mpc}$.
- NGC 4605. This bright Sdm galaxy is situated in the general field between the M81 group and CVn I cloud. Our ACS observations were pointed on the eastern side of NGC 4605 about 1.5 far from its star-like nucleus. In the ACS field we discover more than 10^5 stars seen in both V and I filters. An overwhelming majority of them belong to the RGB population with TRGB position at I = 24.67, yielding the galaxy distance to be 5.47 Mpc.
 - HIPASS J1247-77. This is a dIr galaxy found in the HIPASS blind survey (Kilborn

et al. 2002). The galaxy is situated in the zone of strong extinction, E(B-V)=0.75, and its CMD is heavily contaminated by Milky Way stars. The CM diagram derived by us for the stars located only within the optical boundary of the galaxy (see Fig. 5) reveals the red giant branch population with the TRGB position at $I=24^{\rm m}9$, corresponding to the distance of 3.16 Mpc. In our list, HIPASS J1247-77 is the only galaxy originally discovered in the HI line, but its global parameters: $M(HI)/L_B=0.20$ and $M_{25}/L_B=1.0$ in solar units do not distinguish it from other dIr galaxies.

UGC 8215. This dIr galaxy in the CVn I cloud was resolved into stars for the first time by Makarova et al. (1997), who estimated its distance to be 5.6 Mpc via the brightest stars. The CM diagram derived from our ACS data yields the TRGB distance of 4.55 Mpc which does not change its membership in the CVn I cloud.

UGC 8638. This is another compact irregular galaxy in the direction of the CVn I cloud. Because of the presence in UGC 8638 of bright compact stellar associations, Makarova et al. (1998) were able to determine only the lower limit to its distance, D > 2.3 Mpc. Our ACS photometry of UGC 8638 yields the TRGB distance 4.27 Mpc, typical for the CVn I cloud.

KK 230 = KKR 3. This dIr galaxy of very low surface brightness is one of the faintest ones among the known galaxies of the general field. Our ACS photometry yields for KK 230 the TRGB distance of 1.92 Mpc in agreement with a previous TRGB estimate, 1.90 Mpc, obtained by Grebel (personal communication) from observations with the 10-m Keck telescope. We also performed surface photometry of the galaxy based on its ACS images and derived the galaxy magnitude $I(R < 40'') = 15.6 \pm 0.11$, the integrated color (V - I) = 0.90 inside the same radius R, the central I band surface brightness $22.9 \pm 0.2^m/\Box''$, and the exponential profile scale $(13.4 \pm 0.1)''$. Assuming for KK 230 a typical color (B - V) = 0.50, we estimate its integrated blue magnitude to be $B = 17.0 \pm 0.25$, yielding the absolute magnitude $M_B = -9.47$. Then, the hydrogen mass-to-luminosity ratio and the indicative mass-to-luminosity ratio are 2.3 and 3.3 in solar units, respectively.

IC 4662. This is an isolated dwarf galaxy of high surface brightness with star formation complexes especially prominent at the northern galaxy side. We measured for IC 4662 the TRGB distance to be 2.44 Mpc. That makes this galaxy the nearest known representative of BCD objects. It is amazing that this bright ($B = 11^{\text{m}}.74$) galaxy with the radial velocity of $V_{LG} = 145 \text{ km s}^{-1}$ was never resolved into stars before.

KK 246 = ESO 461-036. The irregular galaxy of low surface brightness is the most isolated system in the Local Volume. Being at the TRGB distance of 7.83 Mpc, KK 246 is situated just at the edge of the Local Void described by Tully (1988). Nevertheless, the

global parameters of KK 246: $M(HI)/L_B = 2.4 M_{\odot}/L_{\odot}$ and $M_{25}/L_B = 4.7 M_{\odot}/L_{\odot}$ do not distinguish KK 246 from other dIrs situated in the known nearby groups.

4. Peculiar velocities of nearby galaxies

A significant part of the scatter of nearby galaxies in the Hubble diagram (Fig. 1) is caused by the virial motions in groups. According to Karachentsev (2005), the meansquare virial velocity of galaxies along the line of sight in 9 nearby groups ranges from 54 km s⁻¹ (IC 342 group, Sculptor filament) to 105 km s⁻¹ (Cen A group) with the median $\sigma_v = 71 \text{ km s}^{-1}$. To study properties of peculiar velocities of the field galaxies themselves, we refined the sample of LV galaxies to exclude group members, keeping only galaxies with the tidal index TI < 0. By the definition of TI (Karachentsev et al. 2004), such a galaxy has a crossing time with respect to its significant neighbor larger than the cosmic expansion time, H^{-1} . For each of these 110 field galaxies, we determined an individual Hubble ratio, $H_i = (V_{LG})/D$. The distribution of this parameter for the LV galaxies is presented in the left panel of Fig. 6. Typical errors on radial velocities ($< 5 \text{ km s}^{-1}$) do not appreciably distort this distribution. The bulk of galaxies on the histogram follow a Gaussian distribution with the mean $\langle H \rangle = 68 \text{ km s}^{-1} \text{ Mpc}^{-1}$ and the standard deviation $\sigma(H) = 15 \text{ km s}^{-1}$ Mpc⁻¹ that is 2.2 times larger than the expected scatter caused by 10% errors in distance measurements. On the left shoulder of the histogram, we recognize an excess number of galaxies with $H = (8 - 32) \text{ km s}^{-1} \text{ Mpc}^{-1}$.

Adopting the mean Hubble parameter for the LV galaxies to be 68 km s⁻¹ Mpc⁻¹, we obtain a distribution of the peculiar velocities of nearby isolated galaxies, $V_{pec} = V_{LG} - \langle H \rangle D$, seen on the right panel of Fig. 6. Again, the number galaxy distribution can be described by a Gaussian law with $\sigma(V_{pec}) = 63$ km s⁻¹ and an asymmetric tail extended far towards negative values.

Apart from 110 isolated LV galaxies with accurate distance estimates via cepheids or TRGB, we added to histograms in Fig. 6 five galaxies, which were listed in Table 3 of CNG as distant objects with low radial velocities. Distances to these galaxies were estimated by less precise methods (from surface brightness fluctuations, SBF, Tully-Fisher relation, TF, or luminosity of the brightest stars, BS). Distance estimates for these galaxies are greater than 10 Mpc, but their radial velocities satisfy a condition $V_{LG} < 500 \text{ km s}^{-1}$. Basic parameters of these are listed in Table 2. Besides NGC 1400, situated in the Eridanus group, the others look to be quite isolated objects. They all are placed in Fig. 6 as the extreme cases with $H < 32 \text{ km s}^{-1} \text{ Mpc}^{-1}$ or $V_{pec} < -500 \text{ km s}^{-1}$.

Different reasons can cause the observed asymmetric distribution of galaxies on their peculiar velocities with a skewness toward negative values. An anisotropy of the Local Hubble flow found by Karachentsev & Makarov (1996, 2001) is among them. The main feature of this phenomena is the low local Hubble parameter value seen in directions toward the poles of the Local Supercluster. Such an effect is expected because of gravitation decelerating of galaxies ofset from the main (most dense) plane of the Supercluster. The character of the local anisotropy is seen in Fig. 7, which displays peculiar velocities of galaxies versus the elevation above the Supergalactic plane as an angle SGB (left panel) and in megaparsecs as SGZ (right panel). In spite of a considerable scatter of galaxies on the diagrams (caused, in particular, by a residual anisotropy of the Hubble flow within the Supergalactic plane), the trends of V_{pec} with SGB and SGZ are clearly seen. The regression $< V_{pec} |SGB>$ has a slope (-2.5 ± 0.5) km s⁻¹deg⁻¹, and the regression $< V_{pec} |SGZ>$ is characterized by a slope (-43 ± 4) km s⁻¹ Mpc⁻¹. The last quantity is of order of the Hubble parameter, meaning that the local anisotropy on Z-coordinate, $d|V_{pec}|/dZ=-0.6 < H>$, turns out to be rather significant.

The distribution on the sky of nearby galaxies with large negative peculiar velocities looks very clumpy. Among ten galaxies with moderate peculiar velocities, [-200, -500] km s⁻¹, seven: UGC 3755, DDO 47, KK 65, UGC 4115, D564-08, D634-03, and D565-06 are situated in a filament aligned along 25° in SGB in the Gemini – Cancer constellations. Moreover, six of the seven galaxies with $V_{pec} < -500$ km s⁻¹ are concentrated within a small ring of radius 5° in the Coma constellation just at the Supergalactic equator. Four of these 6 are superposed on the Coma I group, a region of 5 x 5° around NGC 4494 identified as group 14-1 in the Nearby Galaxies Catalog (Tully 1987). This tight group of early-type galaxies at a distance of 16 Mpc (Tonry et al. 2001) has a mean heliocentric velocity of 902 km s⁻¹. Its dispersion of 283 km s⁻¹ has the consequence that several of its members scatter into our $V_{LG} < 550$ km s⁻¹ sample.

Figure 8 presents a distribution of the distances and peculiar velocities of nearby galaxies. Two straight lines, symmetric with respect to $V_{pec}=0$, indicate a sector of 10% errors in galaxy distance estimates. It is seen that about 2/3 of the galaxies are situated outside this sector. The inclined solid line indicates a zone of observational selection corresponding to $V_{LG}=550~\rm km~s^{-1}$: galaxies without individual distance estimates were included into the CNG only if their corrected radial velocities do not exceed 550 km s⁻¹. Therefore, one may expect the existence of populations of other galaxies, like NGC 925, which have $V_{LG}>550~\rm km~s^{-1}$, but $D<10~\rm Mpc$.

5. Concluding remarks

In the Catalog of 451 LV galaxies (CNG), there are only 214 galaxies with precise distance estimates from luminosities of cepheids and the TRGB, including our present ACS observations of 25 galaxies. Among these, we find a few galaxies whose radial velocities differ from the expectations of a homogeneous isotropic Hubble flow. Considering the sample of 110 LV galaxies that have accurate distance estimates and are situated outside known nearby groups, we derive the mean value of a local Hubble constant to be 68 km s⁻¹ Mpc⁻¹ and the 1D peculiar velocity dispersion of $\sigma_v = 63$ km s⁻¹. Part of this velocity dispersion is caused by anisotropy of the local Hubble flow since the rate of expansion along the Local Supercluster poles is about half that in the LSC plane.

The all-sky distribution of nearby galaxies with high peculiar velocities is unusual. A majority of galaxies with $-500 < V_{pec} < -200$ km s⁻¹ are situated in Gemini – Cancer constellations, forming a filament of $\sim 25^{\circ}$ length along an SGB meridian. This area lies in the region of the 'Leo Spur' in the nomenclature of the Nearby Galaxies Catalog (Tully 1987), the most pronounced part of the 'Local Velocity Anomaly' (Tully, Shaya, and Pierce 1992). In the model presented by those authors, the Leo Spur is converging on the filament in which we live, the two structures drawn together by their mutual attraction. The Gemini – Cancer region is located within the zone of a systematic "blind" survey in the HI line at Arecibo (the project ALFALFA, Giovanelli et al. 2005). This deep survey likely will discovery more objects within the region of the Local Velocity Anomaly.

If one looks around the sky for all galaxies with $V_{pec} < -500$ km s⁻¹, excluding the well-known cases that lie in the Virgo and Fornax clusters, one currently finds 7 examples. Four of these (NGC 4150, UGC 7131, IC 779, KK 127) lie in the tight knot of early type galaxies around NGC 4494 commonly called the Coma I group. One (NGC 1400) is in a similar knot of early type galaxies around NGC 1407 (Gould 1993). Another (UGC 7321) can probably be attributed to backside infall into the Virgo Cluster. The remainder (UGC 6782) may likewise be attributed to Virgo infall or may be assigned a large peculiar velocity due to a falacious distance.

Perhaps it is surprising that there are so few systems with large anomalous velocities. Those few are in very small sectors of the sky and almost all are projected onto the nearest important knots of early-type systems; regions of high inferred mass concentration. The intermediate amplitude peculiar velocities in the Gemini - Cancer constellations appear to be reflections of large-scale streaming; in this case, probably the result of the attraction between the nearest pair of filaments, each with masses in the range of $10^{14} M_{\odot}$ (Tully et al. 1992). Otherwise, galaxy velocities are remarkably quiet about the local expansion, with rms random motions only $\sim 60 \text{ km s}^{-1}$.

Support associated with HST program GO–9771 was provided by NASA through a grant from the Space Telescope Science Institute, which is operated by the Association of Universities for Research in Astronomy, Inc., under NASA contract NAS5–26555. This work was also supported by RFFI grant 04–02–16115.

REFERENCES

Baryshev Yu.V., Chernin A.D., Teerikorpi T., 2001, A&A, 378, 729

Begum A., Chengalur J.N., Karachentsev I.D., 2005, A&A, 433L, 1

Bellazzini M., Ferraro F.R., Pancino E., 2001, ApJ 556, 635

Caldwell, N., Armandroff, T.E., Da Costa, G.S., & Seitzer, P. 1998, AJ, 115, 535

Chernin A.D., 2001, Physics-Uspekhi, 44, 1099

Da Costa G.S., Armandroff T.E., 1990, AJ 100, 162

Ferrarese L., et al. 2000, ApJ 529, 745

Giovanelli R., Haynes M.P., Kent B.R. et al. 2005, AJ (accepted)

Gould, A., 1993, ApJ, 403, 37

Governato F., Moore B., Cen R. et al. 1997, NewA, 2, 91

Huchtmeier, W.K., Karachentsev, I.D., & Karachentseva, V.E. 2001, A&A, 377, 801

Huchtmeier W.K., Skillman E.D., 1998, A&AS, 127, 269

Karachentsev I.D., 2005, AJ, 129, 178

Karachentsev I.D., Karachentseva V.E., Huchtmeier W.K., Makarov D.I., 2004, AJ, 127, 2031

Karachentsev, I.D., Sharina, M.E., Dolphin, A.E. et al. 2003a, A&A, 398, 467

Karachentsev I.D., Sharina M.E., Dolphin A.E., Grebel E.K., 2003b, A&A, 408, 111

Karachentsev, I.D., Makarov, D.I., Sharina, M.E. et al. 2003c, A&A, 398, 479

Karachentsev, I.D., & Makarov, D.I. 2001, Afz, 44, 5

Karachentsev, I.D., Drozdovsky, I., Kajsin, S., et al. 1997, A&AS 124, 559

Karachentsev, I.D., & Makarov, D.I. 1996, AJ, 111, 535

Kilborn, V.A., Webster, R.L., Staveley-Smith, L. et al. 2002, AJ, 124, 690

Lee, M.G., Freedman, W.L., & Madore, B.F. 1993, AJ, 106, 964

Lynden-Bell D., 1981, Observatory, 101, 111

Maccio A.V., Governato F., Horellou C., 2005, MNRAS, 359, 941

Makarova, L.N., Karachentsev, 2003, Astrofizica, 46, 181

Makarova, L.N., Karachentsev, I.D., Takalo, L. et al. 1998, A&AS, 128, 459

Makarova, L.N., Karachentsev, I.D., & Georgiev, Ts.B., 1997, AstL, 23, 378

Saha, A., Claver, J., & Hoessel, J.G. 2002, AJ, 124, 839

Sakai S., Madore B.F., Freedman W.L., 1996, ApJ 461, 713

Sakai S., Ferrarese L., Kennicutt R.C., Saha A., 2004, ApJ, 608, 42

Sandage A.R., 1986, ApJ, 307, 1

Sandage A., Tammann G.A., Hardy E., 1972, ApJ, 172, 253

Schlegel, D.J., Finkbeiner, D.P., & Davis, M., 1998, ApJ, 500, 525

Schombert, J.M., Pildis, R.A., & Eder, J.A. 1997, ApJS, 111, 233

Shaya E., Peebles P.J.E., & Tully R.B., 1995, ApJ, 454, 15

Sirianni M., Jee M.J., Benitez N. et al., 2005, PASP (in press)

Taylor C.N., Thomas D.L., Brinks E., Skillman E.D., 1996, ApJS, 107, 143

Tikhonov, N.A., & Karachentsev, I.D. 1998, A&AS, 128, 325

Tonry, J.L., Dressler, A., Blakeslee, J.P. et al. 2001, ApJ, 546, 681

Tully R.B., 1982, ApJ, 257, 389

Tully, R.B. Nearby Galaxy Catalog, Cambridge Univ. Press, 1987

Tully R.B., Shaya, E.J., & Pierce, M.J., 1992, ApJS, 80, 479

- Fig. 1.— The radial velocity distance relation for nearby galaxies with accurate distance estimates. Members of the M 81 group and Cen A group at ~ 3.8 Mpc are shown as open circles. The galaxies in other nearby groups are indicated as open squares. The field galaxies with the tidal index TI ; 0 are presented as filled circles. The solid line corresponds to the Hubble relation with $H_0 = 68$ km s⁻¹ Mpc⁻¹, curved at small distances because of the decelerating gravitational action of the Local Group assuming a total mass of $1.3 \times 10^{12} M_{\odot}$.
- Fig. 2.— Completeness as a function of magnitude for the least crowded (KK230) and the most crowded (NGC247) objects.
- Fig. 3.— Mean error as a function of magnitude for KK230 and NGC247.
- Fig. 4.— ACS images of 25 nearby galaxies produced by two 600 second exposures in F606W ("V").
- Fig. 5.— ACS color-magnitude diagrams for 25 nearby galaxies. For the small-angular-size galaxy HIPASS1247-77 the CMD is given for the stars inside its optical boundary only.
- Fig. 6.— Number of nearby field galaxies as a function of individual Hubble parameter (left panel) and peculiar velocity, $V_{pec} = V_{LG} 68D$ (right panel).
- Fig. 7.— Peculiar velocity as a function of the Supergalactic latitude (left panel) and distance from the Supergalactic plane (right panel).
- Fig. 8.— Peculiar velocity of nearby field galaxies as a function of distance.

This preprint was prepared with the AAS IATEX macros v5.2.

Table 1. New distances to nearby galaxies

Name	RA(J2000.0)Dec	V_{LG}	I(TRGB)	N_{**}	A_I	$(m - M)_0$	D
		${\rm km~s^{-1}}$	mag		mag	mag	Mpc
E349-031,SDIG	000813.3-343442	216	23.50	13 990	0.02	27.53	3.21
N247	004708.3 - 204536	215	23.80	174560	0.04	27.81	3.65
KKH6	013451.6 + 520530	270	24.49	8 150	0.68	27.86	3.73
UA86	035949.5 + 670731	275	25.14	$69\ 260$	1.83	27.36	2.96
UA92	043200.3 + 633650	89	24.88	30 840	1.54	27.39	3.01
E121-20,KKs19	061554.5-574335	309	24.94	9 350	0.08	28.91	6.05
KKH37	064745.8 + 800726	204	23.75	10 900	0.15	27.65	3.39
E059-01	073119.3 - 681110	245	24.53	$42\ 050$	0.28	28.30	4.57
DDO52	082828.5 + 415124	398	26.08	9 950	0.07	30.06	10.28
D564-08	090254.0 + 200431	365	25.69	3 070	0.05	29.69	8.67
D634-03	090853.5 + 143455	173	25.90	1 860	0.07	29.90	9.46
D565-06	091929.4 + 213612	386	25.82	2670	0.08	29.79	9.08
IKN	100805.9 + 682357	_	23.94	19 230	0.27	27.87	3.75
HS117	102125.2 + 710658	116	24.16	5 890	0.22	27.99	3.96
N4068	120402.4 + 523519	290	24.16	75 830	0.09	28.17	4.31
N4163	121208.9+361010	164	23.35	68 180	0.04	27.36	2.96
U7242,KKH77	121407.4 + 660532	213	24.66	$28\ 240$	0.04	28.67	5.42
IC779, U7369	121938.8 + 295259	198	26.3:	2 100	0.03	30.32	11.6
N4605	124000.3+613629	276	24.67	80 930	0.03	28.69	5.47
HIPASSJ1247-77	124732.6 - 773501	155	24.9	2 560	1.44	27.50	3.16
U8215	130803.6+464941	297	24.26	7 780	0.02	28.29	4.55
U8638	133919.4+244633	$\frac{1}{273}$	24.13	29 850	0.03	28.15	4.27
KK230	140710.7 + 350337	$\frac{126}{126}$	$\frac{22.40}{2}$	$\frac{1}{4} \frac{1}{040}$	0.03	$\frac{26.42}{26.42}$	1.92
IC4662	174706.3 - 643825	145	23.02	$167\ 770$	0.13	26.94	2.44
KK246,E461-36	200357.4 - 314054	401	26.0:	2 990	0.58	29.47	7.83

Table 2. List of distant galaxies with low velocities

Name	RA(J2000.0)Dec	V_{LG} km s ⁻¹	$D \\ \mathrm{Mpc}$	$V_{pec} \ \mathrm{km\ s^{-1}}$	Distance reference
N1400 U6782 U7131 N4150 KK127 U7321	033930.6-184115 114857.3+235016 120911.8+305425 121033.6+302406 121322.7+295518 121734.1+223222	485 452 226 198 105 345	26.4 14.0 14.0 13.7 13.0 20.0	$ \begin{array}{r} -500 \\ -726 \\ -733 \end{array} $	SBF, Tonry et al. (2001) BS, Makarova et al. (1998) BS, Makarova et al. (1998) SBF, Tonry et al. (2001) SB vs. Lumin., present paper IR-TF, present paper

This figure "fig1.gif" is available in "gif" format from:

This figure "fig2.gif" is available in "gif" format from:

This figure "fig3.gif" is available in "gif" format from:

This figure "fig4a.gif" is available in "gif" format from:

This figure "fig4b.gif" is available in "gif" format from:

This figure "fig4c.gif" is available in "gif" format from:

This figure "fig4d.gif" is available in "gif" format from:

This figure "fig4e.gif" is available in "gif" format from:

This figure "fig4f.gif" is available in "gif" format from:

This figure "fig4g.gif" is available in "gif" format from:

This figure "fig5a.gif" is available in "gif" format from:

This figure "fig5b.gif" is available in "gif" format from:

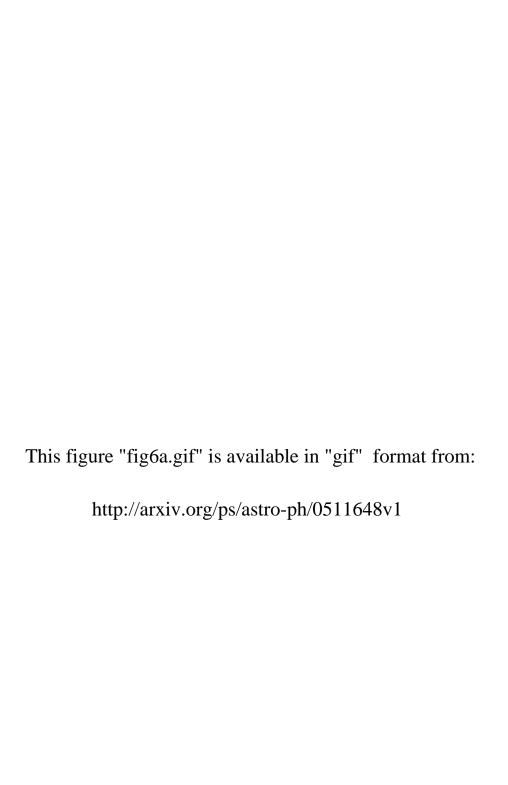
This figure "fig5c.gif" is available in "gif" format from:

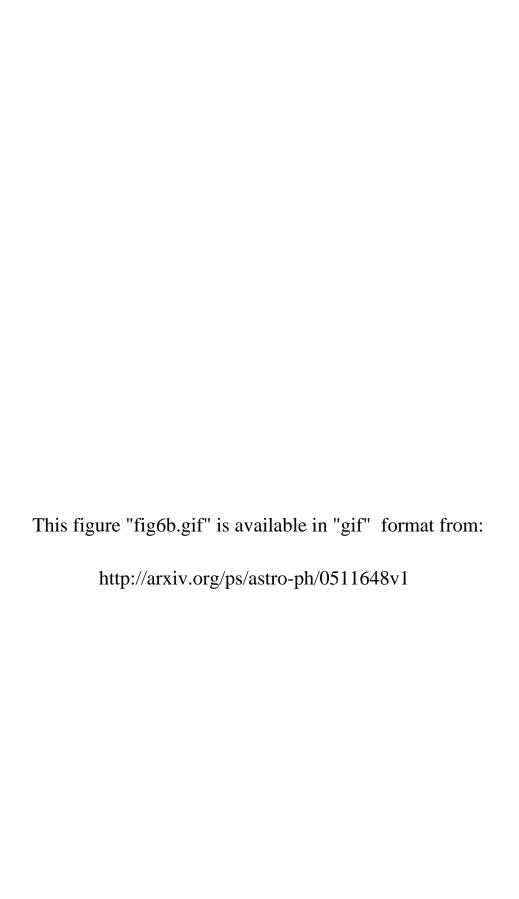
This figure "fig5d.gif" is available in "gif" format from:

This figure "fig5e.gif" is available in "gif" format from:

This figure "fig5f.gif" is available in "gif" format from:

This figure "fig5g.gif" is available in "gif" format from:





This figure "fig7a.gif" is available in "gif" format from:

This figure "fig7b.gif" is available in "gif" format from:

This figure "fig8.gif" is available in "gif" format from: